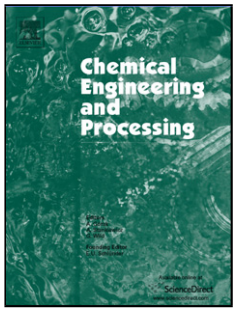

Title: On the bubble-surfactant interaction

Authors: Tadej Stepišnik Perdih, Brane Širok, Matevž Dular

PII: S0255-2701(17)30646-3
DOI: http://dx.doi.org/10.1016/j.cep.2017.08.016
Reference: CEP 7062

To appear in: *Chemical Engineering and Processing*

Received date: 6-7-2017
Revised date: 25-8-2017
Accepted date: 28-8-2017

Please cite this article as: Tadej Stepišnik Perdih, Brane Širok, Matevž Dular, On the bubble-surfactant interaction, Chemical Engineering and Processinghttp://dx.doi.org/10.1016/j.cep.2017.08.016

On the bubble-surfactant interaction

Tadej Stepišnik Perdih (corresponding author)

Faculty of Mechanical Engineering

University of Ljubljana

Askerceva 6, 1000 Ljubljana, SI-Slovenia

E-mail: tadej.stepisnik@fs.uni-lj.si

Phone: +386 1 4771 453

Fax: +386 1 2518 567

Brane Širok

Faculty of Mechanical Engineering

University of Ljubljana

Askerceva 6, 1000 Ljubljana, SI-Slovenia

Matevž Dular

Faculty of Mechanical Engineering

University of Ljubljana

Askerceva 6, 1000 Ljubljana, SI-Slovenia

E-mail: matevz.dular@fs.uni-lj.si

Phone: +386 1 4771 453

Fax: +386 1 2518 567

Graphical abstract

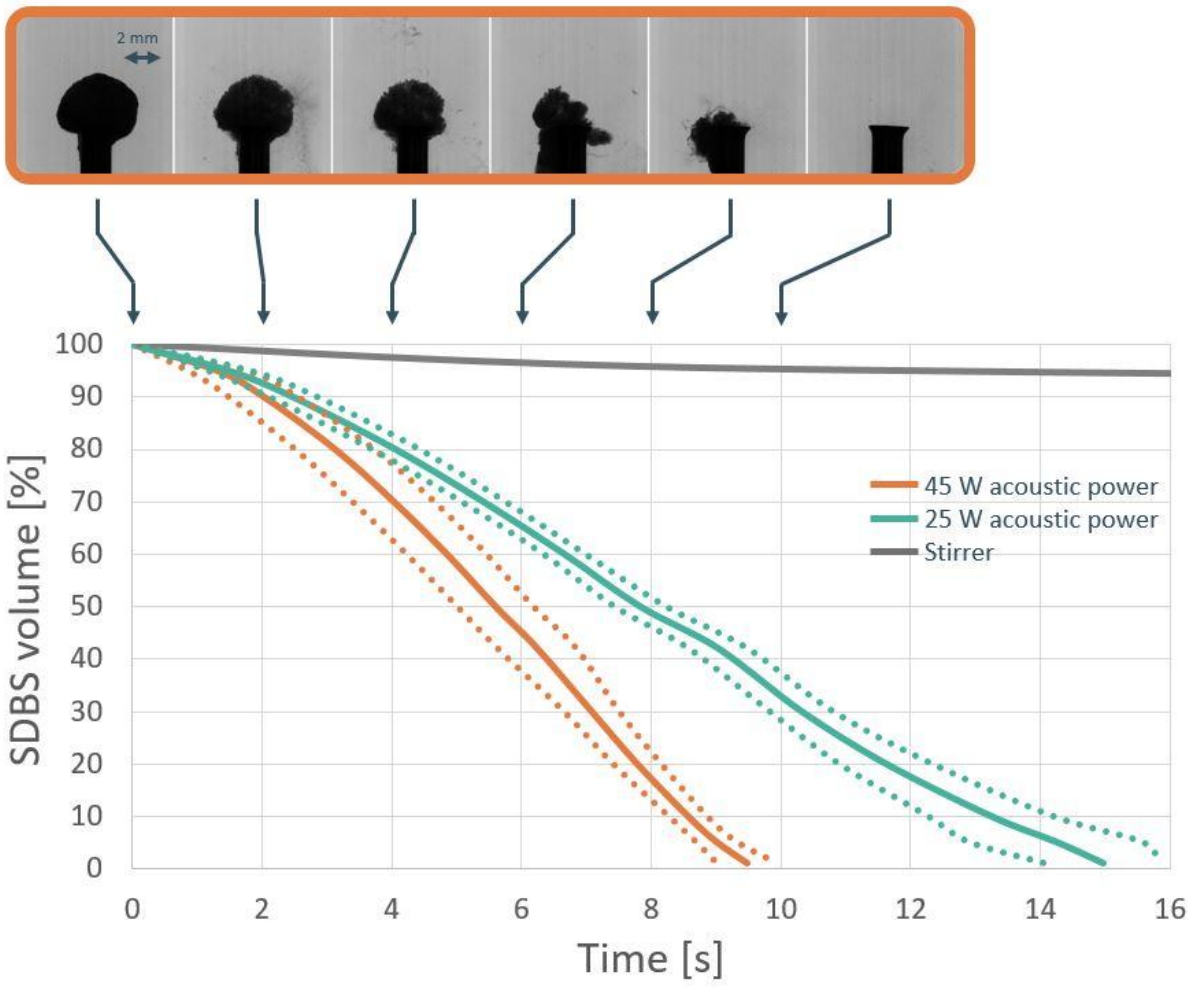

Highlights

- We show how the bubbles interact with surfactant grain
- The physics of dissolution by cavitation resembles the one of cavitation erosion
- Cavitation assisted dissolution can be exploited in household appliances

Abstract

Surfactants play an important role in numerous chemical applications. Their effects on dispersion systems, as emulsions and colloids, are vastly studied. Yet, the dissolution (kinetics) of surfactants themselves has not received much scientific attention, despite the high implications for industrial applications. Nevertheless one can acknowledge the rapid growth of new technologies which are being considered to enhance various chemical processes, one being cavitation – the rapid growth and collapse of vapor bubbles, which results in the formation of shockwaves, streaming, free radicals, high local temperatures etc..

In this paper, we investigate the influence of cavitation on the dissolution rate of Sodium Dodecyl Benzene Sulfonate. Using a high-speed camera, we determined the physics of the dissolution process. We have shown that the presence of cavitation greatly enhances the dissolution rate of surfactant in water through a process comparable to cavitation erosion. Finally, based on our findings, we also present the newly developed cavitation reactor, which could be potentially used for enhancing the process of washing powder dissolution in home appliances.

Keywords: Cavitation, Surfactant, SDBS, Dissolution, High-speed camera, Ultrasound, Bubbles

1 Introduction

Surface active agents, or surfactants as they are named in short, are among the most versatile materials in chemical and process industry [1]. Its amphiphilic nature, containing both hydrophilic and lipophilic functional groups in one molecule, exhibit fascinating interfacial behaviour. Their use is crucial for countless applications and processes, ranging from

pharmaceuticals, petroleum industry, mining and metal industry, paints, cosmetics, cleaning, etc. [2].

Additionally, surfactants are indispensable in the laundry process. They are essential for soil detachment from textile as well as for stabilizing washing solution (entrapping soil) and therefore preventing re-deposition of soil back on fabric [3]. For this reason, surfactant concentration in laundry detergent formulations is in the range 10-40% [4].

While the mechanism of textile washing, depending on the type of soil, type of textile fibre and detergent composition is well understood [1–5], the preparation of the detergent has received only a little attention or researchers. This can lead to over- or under-estimation of appropriate washing time. Too short time can decrease the laundry efficiency and detergent residuals can remain on the textile even after washing. Too long dissolution time consequently leads to too high energy consumption. Considering that laundry machines are globally among the most common household devices, the economic and environmental "cost" of such misjudgement is high!

One of the current attractive ideas for optimization of dissolution process is its acceleration by cavitation – a process of bubble formation due to local depressurization. The process is similar to boiling but much more rapid and aggressive. It can be achieved by introduction of acoustic waves – ultrasonic cavitation or by increasing the velocity of the liquid flow – hydrodynamic cavitation. The basic physics of both are the same on a small scale, but the latter can be more efficiently exploited, mainly due to its continuous nature. At the end of the process, when the bubble enters a higher-pressure region, it violently collapses, causing damage to the solid

surfaces, noise, local increase of temperature, shock waves, micro-jets, vibration and even radical formation and pyrolysis. Although the process is mainly considered as unwanted it can be applied to enhance the performance of many processes, provided it is well understood and controlled [6].

Most of the scientific research of cavitation in the field of dispersion systems is done on micro-mixing [7,8], emulsification and homogenization [9–12]. Cavitation is shown as a very desirable effect on those processes. High shear stresses, elevated turbulence level and microstreaming enhance mass transfer and disrupt the particles or droplets. The mean particle size is the most important parameter to evaluate dispersion quality in those studies. The common conclusion is, that with the application of ultrasound, the size of emulsions/particles is much smaller than with mechanical agitation under the same conditions [13–15]. Dissolution kinetics - our core interest, however, is not in focus of papers listed in this paragraph.

In the paper, we investigate how bubbles interact with the surfactant grain by exposing it to ultrasonic cavitation. By observing the process with a high-speed camera, we were able to determine the physics of the solution process. Additionally, we show efforts to integrate the gained knowledge into a cavitation reactor where cavitation is achieved by hydrodynamics. The device could be installed into a washing machine to increase its washing and consequently also electrical efficiency.

2 Experimental work

Both, the bubble-surfactant interaction experiments and preliminary tests in cavitation generator were set-up at the facility for studying the exploitation of cavitation at the Faculty of Mechanical Engineering, University of Ljubljana.

2.1 The bubble-surfactant interaction set-up

The most common and reliable approach to study the cavitation process is by visualization, hence a transparent ultrasonic bath was machined. The bottom and the three sides are made of acrylic glass. The last, fourth side is made of stainless steel (Fig. 1). The micrometric movement of stainless steel side is excited by a piezoelectric transducer, emitting ultrasound at 33 kHz. This frequency has been selected based on the fact, that at 33 kHz ultrasonic devices exhibit the most aggressive cavitation [16]. The ultrasonic frequency is carried by a low frequency of 100 Hz, hence it is expected for the bubbles to appear periodically, every 0.01 s. We used the calorimetric method to determine the power of emitted ultrasonic waves [17]. Nominal (full) power of the bath is 45 W and the total volume of the bath is 1.1 L.

Sodium dodecyl benzene sulfonate (SDBS) purchased at Sigma-Aldrich was selected as investigated surfactant. SDBS is the most common surfactant used in laundry detergents [3]. 20 mg ± 5 mg SDBS samples were weighed using a precision scale. To affix the samples to the needle tip, the SDBS sample was hydrated and let to dry in ambient air for 24 h. Afterward, the samples and the needle tip were pressed together between two glass surfaces. This fixed the sample and shaped it in a disc, with the same thickness as the needle - 2 mm and diameter of 5 mm (± 10 %). The disc shape of the surfactant enabled to use the assumption, that the disc face area corresponds to surfactant volume.

Prepared samples were immersed in the center of the ultrasonic bath. The dissolution process was observed by the high-speed camera from the introduction of ultrasound, up to a point when the sample fully dissolved. Dissolution was evaluated for acoustic powers 45 W and 25 W,

corresponding to full-power and approximately half-power of our ultrasonic device. The power of the device does not change the frequency or the size of the bubbles, just their number.

In addition, experiments without cavitation were carried out as a reference. Instead of ultrasonic agitation, the bath was placed on a magnetic stirrer (IKA Labortechnik RCT basic) during these tests. The magnetic stirrer was set to 200 rpm, which was the maximal value, at which the air funnel did reach the sample.

6 experiment repetitions were performed for each of the operating points (45 W acoustic power, 25 W acoustic power and silent runs). All experiments were performed at temperature 22 ± 0.5 °C. A typical experiment lasted about 15 seconds. In that time the temperature change was negligible and no cooling of the bath was required.

2.1.1 Observation techniques

The imaging system consisted of camera Fotron FastCam SA-Z, coupled with Mitutoyo M Plan Apo 5x micro-optics or Nikkor 105 mm F 2.8 macro lens (depending on the region of interest). The illumination was provided by two 50.000 Lumen LED light sources. When observing cavitation, two different illumination arrangements are commonly used. One option is that the cavitation bubbles scatter the light (both the light source and the camera face the same direction as in Fig. 1). Images recorded this way have bright bubbles on a dark background. The second option is that observed bubbles are between the camera and the light source (camera faces the lights). With this arrangement, cavitation bubbles appear dark, while the background is bright. We have run experiments in both arrangements. It turned out that images recorded with dark bubbles proved somewhat easier post-processing for dissolution rate determination, while bright bubble images provided more qualitative information on the interaction with the surfactant grain.

Images were recorded at 1000 frames per second for dissolution rate analysis and at 5000 frames per second for bubble-surfactant interaction observation. The image resolution was 640x512 pixels in both cases, what corresponded to spatial resolution of 10 to 20 μm per pixel, depending on the optics that was used.

2.2 Preliminary tests in cavitation generator

Moreover, we show a possible application of the discussed technique – to use cavitation for intensification of laundry aqueous detergent solution preparation. The experiment was designed to simulate an actual washing machine. Here the experiment and the results are given only in a brief form – a more thorough description of the work can be found in [18].

2.2.1 Set-up

A special rotary hydrodynamic cavitation generator (RHCG) was designed. The detergent dissolution rates were experimentally evaluated, for both cavitation and pure liquid flow regime, on a model washing machine. In addition, tests with a magnetic stirrer were performed as a reference.

The experimental set-up is presented in Fig. 2. Together with the rotary hydrodynamic cavitation generator, the experimental set-up consisted of a closed pressure tank, connection pipes and pressure (ABB 266 ast), flow (Bio-Tech: FCH-C-Ms-N) and temperature sensors (Fluke 51 II). Ports visible in Fig. 2 on the top of pressure vessel are used to fill the set-up with water and detergent. When operating, the mixture exits the vessel at the bottom, then it is led through RHCG, where it is exposed to cavitation. RHCG also serves as a pump. Water

and detergent then flow through the control valve and back to the pressure vessel. The RHCG was driven with a single-phase electromotor, which is already present in most of the washing machines.

The design of the rotary hydrodynamic cavitation generator (Fig. 2, right) follows the basic principles of high shear mixing devices [19], adjusted so that it also generates cavitation. The RHCG is an assembly of rotor and stator discs with special geometry inside the closed chamber. Both the rotor and the stator have diameter 50 mm. They have 12 radial indentations, 3 mm deep and 4 mm wide. A more thorough description can be found in [18].

The tank was filled with 2 liters of water at 23.5 °C. 11 grams of standard IEC-A detergent purchased from WFK Institute, Germany, was added to water and left to be treated by the generator for a specified time. The rotational speed of the generator was set to 7000 rpm, which established a flow rate of 11.3 L/min. In the cavitation regime, the tank was open to atmospheric pressure (101 kPa). The non-cavitating flow regime was achieved by closing the tank air valves and raising the static pressure in the tank to 253 kPa. This way cavitation was suppressed, where other hydrodynamic conditions (the rotational speed and the flow rate) were not altered. A high-speed camera was used in order to monitor cavitation presence.

After treating the sample for the specified time, the detergent solution was poured through the textile filter (IEC 60456 standard filter), so that the undissolved detergent remained on the filter which was left to dry and then weighed with a precision scale.

3 Results

We first discuss visualization results on the bubble-surfactant interaction. After that, we focus on the analysis of the preliminary real-application tests. A comprehensive discussion on the physics of the process is offered in chapter 4.

3.1 Analysis of the bubble-surfactant interaction

A short sequence (one period - 0.01s in all) of the grain, which is exposed to cavitation is shown in Fig. 3. The ultrasonic bath was operating at 45 W power and image acquisition frame rate was 1000 fps.

The diameter of the grain is approximately 5 mm. One can see that the cavitation appears at a frequency of 100 Hz, which corresponds to the carrying frequency of the ultrasound. The structures observed here are the so-called streamers [20] - relatively linear streaks of bubbles that travel rapidly from one end to the other, forming a directed bubble stream, which ends at the surface of the grain. Streamer structure represents a constant "supply" of bubbles, which collapse in the vicinity of the grain and cause its rapid dissolution.

A further sequence (Fig. 4) shows the same grain as in Fig. 3, but this time only every 1000^{th} image is shown, thus showing the long term effect of cavitation activity.

At time 0 s, the initial state, prior to application of ultrasound, is shown. The grain has a form of a 2 mm thick disc and has a diameter of roughly 5 mm. Even after only 1s of exposure to cavitation one can see evidence of bubble activity. A comparison of the most affected region of

the grain (its right side in Fig. 4) with the cavitation activity in Fig. 3 confirms that the dissolution is more intense in regions, where cavitation appears. This implies that it can indeed be used for process intensification.

Using image analysis, and the somewhat rude approximation that the grain will maintain its thickness (2mm), one can relatively easily determine its volume function of time. Typical time series of SDBS grain dissolution is presented in Fig. 5 - the diagram corresponds to the case shown in Fig. 4.

The analysis tends to slightly over-estimate the size of SDBS grain due to the presence of cavitation structures and the released SDBS in the vicinity of the grain surface. Nevertheless, we can conclude that the process starts out slowly – only a slight decrease in the volume can be seen after the grain is exposed to cavitation for the first one second. Later on, the dissolution process accelerates and reaches a relatively constant rate, which is followed from the 6^{th} second onwards. The grain is fully dissolved after 9.5-second exposure to cavitation.

Figure 6 shows further cases, where we changed the power of the ultrasonic device and also performed a “silent” experiments of dissolution by stirring the bulk fluid by a magnetic stirrer. For the sake of clearer comparison, only averages and deviations of experiments at the same operating conditions are shown. Since the initial size of the grain slightly varied, the actual volumes are divided by the initial volume and given in percentage.

Obviously, cavitation has a decisive role in the dissolution rate of the SDBS grain – in silent experiments where the ultrasound was switched off and the magnetic stirrer was used to convey the water in the tank, the grain volume only insignificantly decreased in the given time frame. As expected the dissolution was faster when the power of the actuator was increased. The relationship seems to be almost linear – when the power was increased from 25 W to 45 W the full dissolution of the grain was achieved in 9.5 s instead of in 15 s. The size variation of the grains was small (< 10 %), hence the effect can indeed be attributed to the effect of more aggressive cavitation.

The dissolution trend, which we have already described before, seems to follow the same pattern (slow beginning followed by acceleration until a constant final rate is achieved) regardless of the power of the actuator, provided that cavitation occurs.

3.2 Results of preliminary tests in cavitation generator

The results of dissolution for the cavitating, non-cavitating operation regimes and operation with the magnetic stirrer are shown in Fig. 7.

One can clearly acknowledge the potential of the introduction of cavitation into the process of washing powder dissolution. When solely magnetic stirrer was used, more than 35% of the powder remained undissolved after 5 minutes of operation. In the same period of time, only about 15 % of the powder remained undissolved in the case of the non-cavitating regime which was significantly lowered when RHCG operated under cavitation (approximately 5% of powder remained).

The difference in dissolution rates is especially evident in the initial stages of experiments. With the cavitation regime, approximately 80 % of the detergent is dissolved within the first few seconds of the RHCG operation. When the RHCG operates at the same rotation frequency but without cavitation, 150 seconds are required to dissolve the same amount of the detergent.

The dissolution trend is very different from the one we have obtained in a single grain and ultrasonic cavitation (Figs. 5, 6). Here we observe a very rapid dissolution rate at the beginning, which then slowly decreases in time. Probably there are two reasons. Firstly, the sample, in this case, contains a large number of grains, therefore, the initial effect, which observed when using ultrasonic cavitation, can not be distinguished. Secondly, shortest time possible, to conduct a reliable measurement, using a hydrodynamic test rig, is 10 seconds, hence the low initial dissolution rate cannot be detected. The dissolution rate then decreases simply because the quantity of still undissolved powder reduces. The exact mechanisms are still to be thoroughly investigated.

4 Discussion

In Fig. 8 we show a sequence, where an interaction between the grain and the cavitation streamer was observed in more detail at high magnification and higher image acquisition rate (5000 fps). The first two rows show the recorded sequence while the bottom one shows the process in a schematic way for the sake of easier interpretation.

Due to the front light illumination technique used in the present case, both the SDBS grain and the bubbles appear white in the images. We can observe the tip of the streamer, which almost

touches the grain (encircled and marked with the solid arrow). A streak of bubbles is convected towards the grain, where they violently implode due to excitation of the ultrasonic waves (image 2 and c). One can clearly observe that after the collapse of the bubble streamer a new jet of supersaturated SDBS moves away from the grain (pictures 3-8 and d) - at the exact spot, where cavitation bubbles interacted with the grain (marked with the dashed arrow). The amount of "newly" dissolved surfactant is increasing at an increasing rate for about 1/1000s picture (6). After this and until the end of the sequence, the amount of newly dissolved surfactant increases slower.

The sequence is a direct prove how the cavitation bubbles cause SDBS dissolution, which is remarkably similar to the process of cavitation erosion – a well-known nuisance in the engineering community. Also, we can conclude that in the absence of cavitation, dissolution process is solely a result of diffusion and is therefore significantly slower.

If one measures the velocity of bubble movement inside the streamer a value between 0.1 and 1 m/s is obtained. This corresponds perfectly with the velocities which were evaluated by [21]. A similar agreement can be found for the bubble size, which lies in the order of about 20μm (an accurate measurement is not possible in the present case, but individual bubbles can barely be resolved – they only occupy a single pixel in the images).

In the present case, we deal with ultrasonic cavitation where the streamer structure – a well-defined streak of bubbles – is generated near nodal zones as a direct result of the primary Bjerknes and the secondary Bjerknes forces [22]. Interestingly a very similar structure was

recently observed in the case of hydrodynamic cavitation by Dular and Petkovsek [23]. It is known as a "twister" and one must emphasize its erosive potential (Fig. 9).

Its origin is in the vortex which forms in the cavity closure (also known as the cavity breakup) region. The vortex first remains liquid but then cavitates as it interacts with a cloud of cavitation nuclei. This interaction focuses streak of bubbles towards the solid material and damages it. It was determined that the majority of the damage is in the region where the twister touches the solid surface and that it generally occurs when the vortex breaks-up.

The streamer, shown in Fig. 8 is roughly 1mm long and has a diameter of 0.1mm. We can estimate the magnitude of the pressure wave, which is emitted at bubble collapse by a simple simulation, using the Rayleigh-Plesset bubble dynamics approach [24]:

$$\rho_l \left(R\ddot{R} + \frac{3}{2}\dot{R}^2 \right) = p_v - p_\infty + p_{g0} \left(\frac{R_0}{R} \right)^{3\gamma} - \frac{2S}{R} - 4\mu \frac{\dot{R}}{R} \quad (1)$$

Further, we can estimate the maximal pressure magnitude by [24]:

$$p_{collapse} = p_\infty + (p_\infty - p_v) \frac{\left(\frac{R_0^3}{4R^3} - 1 \right)^{4/3}}{\left(\frac{R_0^3}{R^3} - 1 \right)^{1/3}} \quad (2)$$

The results are shown in Fig 10.

The simulation shows that an ultrasonic pressure field with a frequency of 33 kHz will force bubbles to follow it. The bubble will periodically undergo a rapid growth and collapse, which will then be followed by a number of rebounds. The process takes place approximately every 33 μs, leading to the estimation of about 300 collapses per period of caring frequency (100 Hz).

Solving the Rayleigh-Plesset equation also gives the maximum size of the bubble in the order of 20 μm – again compiling well to the experiment. By solving Eqn. 2 one can also estimate the amplitude of the pressure wave released at the bubble collapse – approximately 25 MPa in this specific case. This is high enough to damage a soft material or, as in the present case, cause mechanical disruption to the grain structure and consequently "freeing" some of the detergent into the bulk fluid.

As mentioned previously, the dissolution process and time evolution are remarkably similar to the well-known evolution of the material mass loss during cavitation erosion process – Fig. 11.

In cavitation erosion studies, we normally first observe a period, where no mass loss is present – an incubation period. During this time, the surface of the material sustains only microscopic plastic deformation which results in work hardening of the material. When the material is hardened enough, it cannot sustain additional forces from the bubble collapse and small parts of it separate – we enter the acceleration period. During this time, the mass loss rate increases until it reaches the maximum constant value. From this moment onwards, a constant mass loss rate is usually measured, which can somewhat decrease later on.

Since the SDBS grain itself is relatively unstable, the incubation period could not be determined during the present experiments – the dissolution process starts immediately after the piezo actuator is switched on and cavitation forms. The trend then follows the one observed in cavitation erosion – including a slight decrease in the rate by the end of the exposure to cavitation. The maximum constant value of dissolution rate is achieved between 5 and 6 seconds. This value may be influenced by the bulk detergent concentration. The reason may lie in the decreased amplitude of pressure wave at the bubble collapse (lower surface tension will decrease the collapse velocity and the resulting pressure wave amplitude), Concentration could also affect the diffusion of newly dissolved detergent. However, diffusion is much weaker that convection induced by collapsing bubbles and it is unlikely that the process would be governed by the difference of concentration directly.

6 Conclusions

We investigated cavitation-assisted dissolution of a surfactant. Employing high-speed visualization as observation technique gave us a comprehensive insight into physics of the process.

Firstly, we showed, that cavitation immensely improves surfactant dissolution rates in comparison to the magnetic stirrer. It takes roughly 9.5 s for surfactant grain to be dissolved with 45 W acoustic power and 15 s with 25 W acoustic power. Emitted acoustic power has an almost linear effect on dissolution time. In that time only about 5 % of the surfactant grain is dissolved using magnetic stirrer.

Secondly, we analysed the interaction of cavitation bubble and surfactant in more detail. High-resolution images recorded with 5000 fps show streaks of cavitation bubbles called streamers imploding in the vicinity of surfactant. This appears to be the primary mechanism for enhanced dissolution. Solving Rayleigh-Plesset equation we estimated shockwave amplitudes to be in the order of 25 MPa, which is sufficient to disrupt surfactant grain. The whole process has a high resemblance to that of cavitation erosion, which implies that conclusions from the latter research field, which is studied extensively, can be employed for exploiting the process in the former one.

Lastly, we illustrate the industrial potential of cavitation-enhanced dissolution. We designed continuously operating hydrodynamic cavitation reactor to prepare a detergent solution for textile washing. Results indicate that washing time of commercial washing machine could be reduced for roughly 10 minutes using such a device. This could lead to considerable improvements in water and energy consumption. Cavitation reactors could, therefore, be a robust and economic solution for use in laundry appliances.

References

[1] D. Myers, Surfactant science and technology, 3rd. ed., John Wiley & Sons., 2006.

[2] R.J. Farn, Chemistry and Technology of Surfactants, 2007. doi:10.1002/9780470988596.

[3] E. Smulders, W. Rähse, G. Jakobi, Laundry detergents, Wiley-VCH, 2002.

[4] C. a. Miller, K.H. Raney, Solubilization—emulsification mechanisms of detergency, Colloids Surfaces A Physicochem. Eng. Asp. 74 (1993) 169–215. doi:10.1016/0927-7757(93)80263-E.

[5] M.J. Rosen, J.T. Kunjappu, Surfactants and interfacial phenomena, Wiley, 2012.

[6] P.R. Gogate, Cavitational reactors for process intensification of chemical processing applications: A critical review, Chem. Eng. Process. Process Intensif. 47 (2008) 515–527. doi:10.1016/j.cep.2007.09.014.

[7] J. Jordens, B. Bamps, B. Gielen, L. Braeken, T. Van Gerven, The effects of ultrasound on micromixing, Ultrason. Sonochem. 32 (2016) 68–78. doi:10.1016/j.ultsonch.2016.02.020.

[8] M. Rahimi, N. Azimi, F. Parvizian, Using microparticles to enhance micromixing in a high frequency continuous flow sonoreactor, Chem. Eng. Process. Process Intensif. 70 (2013) 250–258. doi:10.1016/j.cep.2013.03.013.

[9] S. Kentish, T.J. Wooster, M. Ashokkumar, S. Balachandran, R. Mawson, L. Simons, The use of ultrasonics for nanoemulsion preparation, Innov. Food Sci. Emerg. Technol. 9 (2008) 170–175. doi:10.1016/j.ifset.2007.07.005.

[10] S.M. Jafari, E. Assadpoor, Y. He, B. Bhandari, Re-coalescence of emulsion droplets during high-energy emulsification, Food Hydrocoll. 22 (2008) 1191–1202. doi:10.1016/j.foodhyd.2007.09.006.

[11] K.A. Ramisetty, A.B. Pandit, P.R. Gogate, Ultrasound assisted preparation of emulsion of coconut oil in water: Understanding the effect of operating parameters and comparison of reactor designs, Chem. Eng. Process. Process Intensif. 88 (2015) 70–77. doi:10.1016/j.cep.2014.12.006.

[12] D. Nagatomo, T. Horie, C. Hongo, N. Ohmura, Effect of ultrasonic pretreatment on emulsion polymerization of styrene, Ultrason. Sonochem. 31 (2016) 337–341. doi:10.1016/j.ultsonch.2016.01.010.

[13] L.C. Hagenson, L.K. Doraiswamy, Comparison of the effects of ultrasound and mechanical agitation on a reacting solid-liquid system, Chem. Eng. Sci. 53 (1998) 131–148.

[14] C. Sauter, M.A. Emin, H.P. Schuchmann, S. Tavman, Influence of hydrostatic pressure and sound amplitude on the ultrasound induced dispersion and de-agglomeration of nanoparticles, Ultrason. Sonochem. 15 (2008) 517–523. doi:10.1016/j.ultsonch.2007.08.010.

[15] M.D. Luque de Castro, F. Priego-Capote, Ultrasound-assisted preparation of liquid samples, Talanta. 72 (2007) 321–334. doi:10.1016/j.talanta.2006.11.013.

[16] ASTM International, ASTM G32 - 16 Standard Test Method for Cavitation Erosion Using Vibratory Apparatus, (2016). doi:10.1520/G0032-16.

[17] T. Kimura, T. Sakamoto, J.-M. Leveque, H. Sohmiya, M. Fujita, S. Ikeda, et al., Standardization of ultrasonic power for sonochemical reaction, Ultrason. Sonochem. 3 (1996) S157–S161. doi:10.1016/S1350-4177(96)00021-1.

[18] T. Stepisnik Perdih, B. Sirok, M. Dular, Influence of Hydrodynamic Cavitation on Intensification of Laundry Aqueous Detergent Solution Preparation, Strojniški Vestn. -

Journal Mech. Eng. 63 (2017) 83–91. doi:10.5545/sv-jme.2016.3970.

[19] J. Zhang, S. Xu, W. Li, High shear mixers: A review of typical applications and studies on power draw, flow pattern, energy dissipation and transfer properties, Chem. Eng. Process. Process Intensif. 57–58 (2012) 25–41. doi:10.1016/j.cep.2012.04.004.

[20] R. Mettin, S. Luther, C.-D. Ohl, W. Lauterborn, Acoustic cavitation structures and simulations by a particle model, Ultrason. Sonochem. 6 (1999) 25–29. doi:10.1016/S1350-4177(98)00025-X.

[21] R. Mettin, S. Luther, W. Lauterborn, Bubble size distribution and structures in acoustic cavitation, in: Proc. 2nd Conf. Appl. Power Ultrasound Phys. Chem. Process., Tolouse (France), 1999: pp. 125–129.

[22] T.G. Leighton, The acoustic bubble, Academic Press, 1994.

[23] M. Dular, M. Petkovšek, On the mechanisms of cavitation erosion - Coupling high speed videos to damage patterns, Exp. Therm. Fluid Sci. 68 (2015) 359–370. doi:10.1016/j.expthermflusci.2015.06.001.

[24] J.-P. Franc, J.-M. Michel, Fundamentals of Cavitation, Kluwer, cop., 2004. doi:10.1007/s13398-014-0173-7.2.

Figure captions:

Fig. 1: Experimental set-up.

Fig. 2: Experimental set-up (left) and the cavitation generator (right, adopted from [18]).

Fig. 3: A sequence showing the dynamics of cavitation in the vicinity of the grain. Time step between images is 1ms.

Fig. 4: Long-term observation of surfactant grain. Time step between images is 1 s.

Fig. 5: Diagram showing grain volume as a function of time of exposure to cavitation.

Fig. 6: Dissolution as a function of time and actuator power. Experiments with the magnetic stirrer are also shown.

Fig. 7: The measurements of the detergent dissolution rate in the prototype of cavitation device (adopted from [18]).

Fig. 8: Sequence showing the interaction between a bubble and the grain.

Fig. 9: Twister cavitation structure (adopted from [23]).

Fig. 10. Simulation of a single bubble dynamics. The bottom diagram shows the ultrasonic pressure field of 30kHz, the upper diagram shows the bubble response to it, while the middle one gives the pressure which is emitted at bubble collapse.

Fig. 11. Left - measured dissolved grain volume and volume dissolution rate (case from Fig. 4) and a typical evolution of material mass loss and material mass loss rate in cavitation erosion (right, adopted from [24]).